Geometric secluded paths and planar satisfiability

Valentin Polishchuk and Leonid Sedov

Communications and Transport Systems, ITN, Linköping University, Sweden firstname.lastname@liu.se

Roman Voronov

 $Institute\ of\ Mathematics\ and\ Information\ Technologies,\ Petrozavodsk\ State\ University,\ Russia\ rvoronov@petrsu.ru$

Abstract

We consider paths with low "exposure" to a polygonal domain, i.e., paths which are seen as little as possible; we differentiate between "integral" exposure (when we care for how long the path sees every point of the domain) and "0/1" exposure (just counting whether a point is seen by the path or not). For the integral exposure, we give a PTAS for finding the minimum-exposure path between two given points in the domain; for the 0/1 version, we prove that in a simple polygon the shortest path has the minimum exposure, while in domains with holes the problem becomes NP-hard. We also highlight connection of the problem to minimum satisfiability and settle hardness of variants of planar min- and max-SAT.

2012 ACM Subject Classification Theory of computation Computational geometry

Keywords and phrases Computational geometry, Visibility, Route planning, Security/privacy, Planar satisfiability

Digital Object Identifier 10.4230/LIPIcs...

1 Introduction and Related work

Both visibility and motion planning are textbook subjects in computational geometry – see, e.g., the respective chapters in the handbook [19] and the books [18,32]. Visibility meets routing in a variety of geometric computing tasks. Historically, the first approach to finding shortest paths was based on searching the visibility graph of the domain; visibility is vital also in computing minimum-link paths, i.e., paths with fewest edges [23,29,30,36]. "Visibility-driven" path planning has attracted also some recent interest [3,34,41]. In addition to the theoretical considerations, visibility and motion planning are closely coupled in practice: computer vision and robot navigation go hand-in-hand in many courses and real-world applications.

The question of "hiding" a path in a polygonal domain was first raised in a SoCG'88 paper [17]: it considered the "robber route problem" in which the goal was to minimize the length traveled within sight of at least one of a number of "threats" (each threat being a point); the problem reduces to finding the shortest path in the $0/1/\infty$ metric that assigns cost of 1 to the union of the visibility polygons of the threats, and 0 to the rest of the domain (the complement of the domain, where travel is forbidden is assigned the infinite weight). Our settings are different from [17] in two aspects: (1) we have a continuum of the threats (every point in the domain is a threat) and (2) in the integral version, we care about "how many" threats are seen from points along the path (formally: we integrate the visible area along the path); in other words, we account for the "intensity" of the visibility from the threats, which may be relevant if every threat is e.g., shooting (or otherwise negatively influencing) the path.

XX:2 Geometric secluded paths and planar satisfiability

	0/1	Integral
	exposure	exposure
With holes	Hard (Thm. 1)	PTAS
Simple	P (Thm. 2)	(Thm. 3)

Table 1 Hardness of minimum-exposure paths in polygonal environments

	min2SAT	max2SAT
V-cycle	Hard (Thm. 6)	
VC-cycle	Open	Hard
Separable	P (Thm. 4)	(Thm. 6)
Monotone	P (Cor. 5)	

Table 2 Hardness on versions of planar opt2SAT (see Section 4 for definitions)

Lately, motivated by the rise of IoT and mobile computing, there has been a surge of research on anonymity, security, confidentiality and other forms of privacy preservation (in particular, in geometric environments [4]), studying paths with minimum exposure to sensors in a network [13,15,35,40]. The standard model, again, assumes a finite number of point sensors, so the visibility is changing discretely, as the path goes in/out of a sensor coverage. To our knowledge, Lebeck, Mølhave and Agarwal [24,25] were the first to introduce integration of the visibility continuously changing along the path (which is also one of our models). Our paper is different from Lebeck et al. in that we give algorithms with provable theoretical performance in continuous domains under the usual notion of distance-independent visibility (Lebeck et al. presented strategies with outstanding practical performance on discretized terrains, in the more realistic model of visibility deteriorating with distance).

Minimizing the integral exposure can be viewed as an extension of the weighted region problem (WRP) [2,7–9,11,21,31,33] to the case of continuously changing weight; in WRP the input is a weighted polygonal subdivision of the domain (with a constant weight assigned to each cell of the subdivision) and the goal is to find the path minimizing the integral of the weight along the path. Computational complexity of WRP is open; PTASes for the problem have running times that depend not only on the complexity of the subdivision, but also on various parameters of the input like ratio of max/min weight, largest coordinate and angles of the regions, etc. (the parameters differ between the algorithms, see [38, Ch. 31] for details). Integration of other measures of "local quality" (different from visibility) for points along a path was the subject also in the study of high-quality paths [1,42] and related research [43,44].

Recent papers [6,16,27,39] explored paths adjacent to few vertices in graphs; such paths were dubbed secluded in [6]. Our paper may thus be viewed as studying geometric versions of the secluded path problem.

Contributions and Roadmap In Section 2 we prove that in a polygonal domain with holes it is NP-hard to find a path, between two given points, minimizing the area seen from the path; the reduction is from minSAT (find the truth assignment to Boolean variables so as to satisfy the minimum number of given disjunctive clauses). In Section 2.1 we complement the hardness by showing that in a simple polygon, shortest paths are the ones that see minimum area. Section 3 gives a PTAS for minimizing the integral of the seen area along the path; we first give a generic scheme for building a piecewise-constant approximation of the visibility area for points in the domain, and then in Section 3.2 present details of an implementation which allows applying a PTAS for WRP on our "pixels" with approximately constant seen area. Finally, in Section 4 we further explore the connection between path hiding and minSAT, and determine hardness of versions of planar minSAT (and maxSAT). Tables 1 and 2 summarize the results.

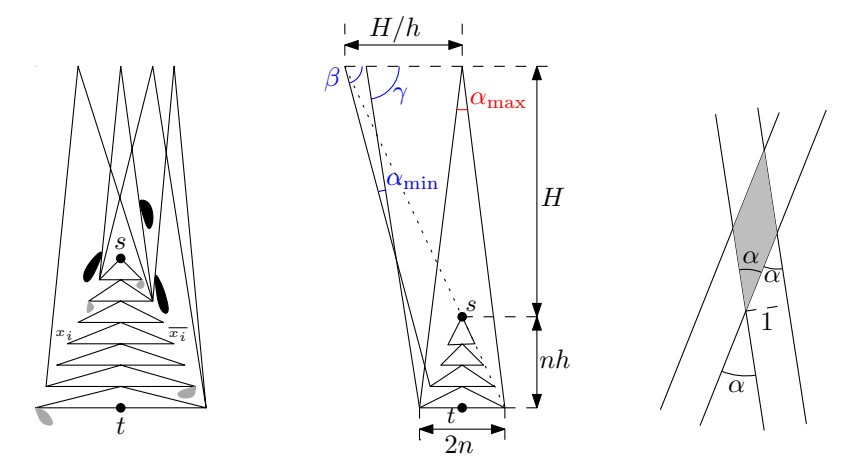


Figure 1 Left: The reduction from min2SAT. All segments are thin corridors of P. Some leakage-blocking high-area chambers are shown black and some area equalizers are shown gray (both black and gray belong to the domain). Middle: the largest angle at a clause and the smallest angle at a midway intersection. The c clauses are spread evenly on the segment of width 2H/h; thus, the distance between clauses (the base of the triangle with angle α_{\min} at the apex) is $\frac{2H}{h(c-1)}$. Right: Midway intersection of unit-width corridors is area- $\frac{1}{\sin \alpha}$ rhombus with side $\frac{1}{\sin \alpha}$ and angle α .

Notation and Problems formulation We use $|\cdot|$ to denote the measure of a set, i.e., length of a segment and area of a 2D set. Let P be a polygonal domain with n vertices and $s,t\in P$ be two given points in it. For a point $p\in P$ let V(p) be the visibility polygon of p, i.e., the set of points seen by p. We study the following problems:

- \blacksquare GEOMETRIC SECLUDED PATH: Find the s-t path that sees as little area of P as possible.
- INTEGRAL GEOMETRIC SECLUDED PATH: Find the s-t path π that minimizes the integral of the area of the visibility polygon over the points along the path, $\int_{\pi} |V(p)| dp$.

2 Minimizing seen area

We prove that exposure minimization is NP-hard in general, but in simple polygons the minimum-exposure path is the shortest path.

▶ **Theorem 1.** Geometric Secluded Path is NP-hard.

Proof. We reduce from min2SAT: find truth assignment for a set of n variables, satisfying the minimum number of given two-literal disjunctive clauses. (Inside this proof n will denote the number of variables and c – the number of clauses.) Figure 1, left illustrates the construction. A variable gadget is an equilateral triangle. The triangles for the variables are stacked into a "Christmas tree", with s and t placed at the top and the root resp. Going through the left (resp. right) vertex of a triangle represents setting the variable to True (resp. False). The clauses are all put on a horizontal line above the Christmas tree so that the segment between any literal and any clause does not intersect the tree. Each clause is connected to its literals, and all connections (including the ones forming the Christmas tree edges) are thin corridors forming the domain; a clause gadget is simply the intersection of the two corridors. The idea of the reduction is to have s-t path go through all variable gadgets, choosing whether to go through the variable or its negation in every gadget: the fewer clause gadgets are seen, the fewer clauses are satisfied.

Few technicalities have to be taken care of:

Two variable-clause corridors, leading to different clauses, may intersect "in the middle" of the corridors, and we have to make sure that the area of such a midway intersection is much smaller than the clause gadget area. Being smaller by a factor $4c^3$ will suffice: even if parts of a corridor are seen due to the midway intersections with all (at most 2c-1) other corridors, the total seen corridor's "midway" area will still be smaller (by a factor $\approx 2c^{\prime}$) than the area of a single clause gadget. Moreover, with such small midway intersections, they may be neglected altogether when counting the areas of clause gadgets seen from literals: the total areas of all (at most $4c^2$ midway intersections) will be smaller (by at least a factor of c) than the area of a single clause gadget. To reduce areas of the midway intersections in comparison to the clause gadgets areas, we put the clause gadgets high above the Christmas tree – at height H, to be determined later (Fig. 1, middle). The area of intersection of two corridors (Fig. 1, right) is inversely proportional to the sine of the angle between the corridors (our corridors are all of the same width), so the smallest-area clause gadget would be the one for the clause $x_n \vee \overline{x_n}$ placed directly above the apex of the Christmas tree (since we do not control which clause goes where on the clauses line, we have to consider the worst case); let α_{max} be the angle between the corridors defining the gadget. Assuming the height of every variable gadget triangle is h and their bases have lengths $2, 4, \ldots, 2n$ (refer to Fig. 1, middle),

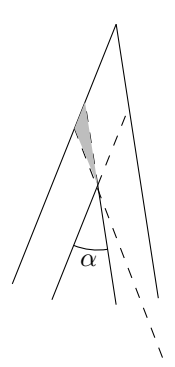
$$\alpha_{\max} = 2\arctan\frac{n}{H+nh}$$

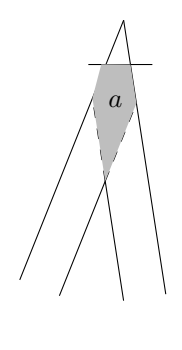
On the other hand, the *smallest* angle between two interesting corridors that do not lead to the same clause (i.e., the smallest angle that may define the area of a midway intersection) can be formed by corridors leading to last and last-but-one clause from the last-but-one and last variables x_n, x_{n-1} resp. (changing the endpoints of the corridors would only increase the angle of intersection); the angle is

$$\alpha_{\min} = \gamma - \beta = \arctan \frac{H + nh}{H/h - \frac{2H}{h(c-1)} - n} - \arctan \frac{H + (n-1)h}{H/h - (n-1)}$$

By trigonometric formulas, the ratio $\sin \alpha_{\min}/\sin \alpha_{\max}$, after being squared a constant number of times, is a ratio of polynomials. A Mathematica script shows that this ratio tends to infinity as H grows (Appendix B gives the Mathematica listing); hence, at a polynomially large H, the ratio becomes larger than $4c^2$, as we need.

- We make sure that the area, around a clause gadget, seen from one literal but not from the other, is negligible in comparison with the clause gadget area (seen from both literals of the clause). This is already taken care of by making the whole construction tall (large H) in the above (Fig. 2, left).
- Leakage of paths from the Christmas tree into variable-clause corridors is prevented by attaching a large-area chamber to each corridor (between the literal and the first intersection of two corridors), so that a path going through the corridor would see the whole area of the chamber. To ensure that the area of a single chamber is larger than the area seen by any path through the Christmas tree, the whole construction is scaled up while keeping the width of the corridors fixed: since the areas available for the chambers grow quadratically with the scaling factor and the areas seen along the corridors grow linearly, a polynomial scaling will suffice to ensure that the chambers areas are large enough to prevent the path going anywhere except through the variable gadgets.
- We attach area equalizers to the literals so that no matter whether the path passes through the variable or its negation, it sees the same non-clause area (the areas may be different between the different variables; we only make sure that for any *single* variable





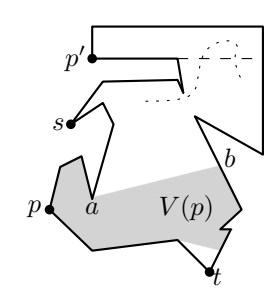


Figure 2 Left: Area seen by one literal only (gray) is negligible for small α . Right: Decreasing clause gadget area.

Figure 3 V(p) is shaded; ab is the essential cut of p. A dotted path, crossing the cut of p' (dashed), can be shortcut along the cut.

the seen non-clause area does not depend on whether the variable is set to true or false by the path).

■ In the construction so far, different clause gadgets may have different areas; let a denote the smallest area of a clause gadget. We make sure that all clause gadgets have area a, which can be done e.g., by appropriately cutting off the clause gadgets from the top (Fig 2, right).

Now, all s-t paths, going through the Christmas tree only, will see the same non-clause area A. The total area seen by a path is then $\approx A + ka$ where k is the number clauses seen by the path, which is the same as the number of clauses satisfied by the truth assignment set by the path (we say that the seen area is approximately equal to A + ka because of the non-counted areas that may be seen—midway intersections and parts seen by one literal only—which we made sure to be negligible in comparison with a).

In Section 4 we discuss why we could not use *planar* min2SAT to prove hardness of Geometric Secluded Path, avoiding dealing with the crossings.

2.1 Simple polygons

We show that in a simple polygon shortest paths see least area:

▶ **Theorem 2.** If P is a simple polygon, the shortest s-t path is the solution to Geometric Secluded Path.

Proof. The visibility polygon V(p) of a point $p \in P$ is bounded by edges and chords of P, with each chord connecting a vertex of the polygon to a point on its boundary. If P is a simple polygon and p does not see s ($s \notin V(p)$), then there is a unique chord separating p from s; the chord is called the essential cut of p [5] (Fig. 3). If an essential cut does not separate s from t, then the shortest s-t path does not cross the cut, for otherwise, the path could be shortcut along the cut. That is, the shortest path crosses those and only those cuts that separate s from t. But any other path also has to cross all such cuts, i.e., has to see all the points seen by the shortest path.

3 A PTAS for minimizing integral exposure

In Section 3.1 we give a generic way to partition the domain so that the visible area is approximately constant within a cell of the partition; then in Section 3.2 we present details

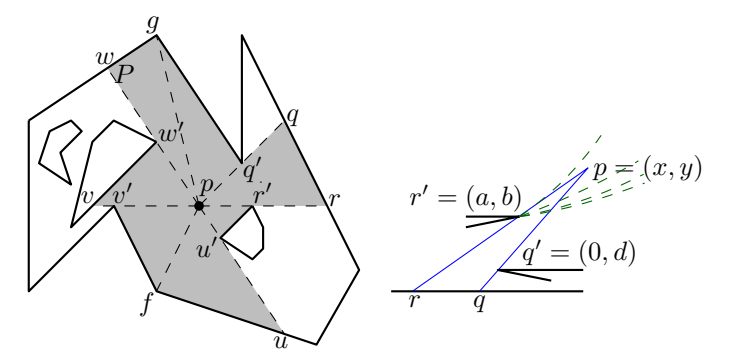


Figure 4 Left: Domain P with 3 holes and a point $p \in P$; V(p) is shaded. Triangle pqr has two rotating sides, triangles puf, pvw', pwg have one fixed-endpoint and one rotating side; the other triangles have two fixed-endpoint sides. Right: |pqr| = y|rq|/2. Green dashed are level sets of |pqr|.

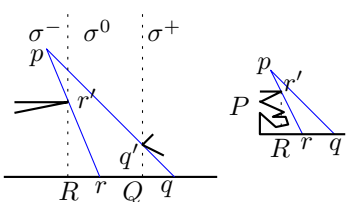


Figure 5 Left: For $p \in \sigma^-$, |r'Rr| is subtracted from C while |q'Qq| is added; for $p \in \sigma^0$, both areas are added; for $p \in \sigma^+$, |r'Rr| is added while |q'Qq| is subtracted. Right: r'R is not fully inside P.

of a slightly different partitioning, having straightline edges, on which a PTAS for WRP can be applied to find the path with approximately minimum integral exposure.

3.1 Reduction to WRP with curved regions

We first compute the visibility graph of P (the graph connecting pairs of mutually visible vertices of the domain) and extend every edge of the graph in both directions maximally within P. The extensions of the visibility edges split P into $O(n^4)$ cells such that the visibility polygon V(p) is combinatorially the same for any point p within one cell of the subdivision; call the subdivision the visibility decomposition of P. In particular, the area |V(p)| is given by the same formula for any point p in one cell σ of the decomposition. Specifically, the rays from p through the seen vertices of P split V(p) into O(n) triangles (Fig. 4, left). The side of any triangle, opposite to p, is a subset of an edge of P; we call this side the base of the triangle. Each of the other, non-base sides is formed by a ray passing through a vertex r' of P and ending at a point r on the base. (In Section 3.2 we will differentiate between fixed-endpoint sides for which r = r' is an endpoint of the base and rotating rays which rotate around r' if p moves; here we treat both types of sides with a single formula, since fixed-endpoint sides may be viewed as a special case of rotating sides with r=r'.) To write the formula for the area of the triangle pqr, we follow [10, Appendix A.1] and assume that the base is the x-axis and that both p = (x, y) and r' = (a, b) lie above the base $(y, b \ge 0)$; then the abscissa of r is x - y(x - a)/(y - b) (Fig. 4, right). Let q' be the vertex that defines the other side, pq, of pqr; to simplify the formulas, assume w.l.o.g. that q' lies on the y-axis: q'=(0,d). The abscissa of q is then x-yx/(y-d), and the area $y|rq|^2$ of the triangle pqr

$$|pqr| = \frac{y^2}{2} \left(\frac{x-a}{y-b} - \frac{x}{y-d} \right) \tag{1}$$

Next, to obtain a piecewise-constant $(1+\varepsilon)$ -approximation of the area |V((x,y))| visible from point $(x,y)\in P$, we use level sets of the area function (1). For a given area A, the equality |pqr|=A is attained along the curve γ_A

$$x = \frac{2A/y^2 + a/(y-b)}{1/(y-b) - 1/(y-d)} \tag{2}$$

Consider a cell σ of the visibility decomposition. We split σ with the curves γ_{A_i} for a set $\mathcal{A}=(A_1,\ldots,A_i,\ldots)$ of areas forming geometric progression with common ratio $1+\varepsilon$: $A_i=(1+\varepsilon)A_{i-1}$. Let S_i denote the set of points p for which the area of the triangle pqr is between A_{i-1} and A_i (that is, $S_i=\{p\in\sigma:A_{i-1}<|pqr|\leq A_i\}$ are the points between $\gamma_{A_{i-1}}$ and γ_{A_i}). We call S_i a curved sector because in equation (2), x(b)=a for any A, i.e., all curves γ_A have r'=(a,b) as a common point. (We put a GeoGebra graphics to play with the level sets to see how they look at https://www.geogebra.org/graphing/cvxvhfcf.) We assign the same weight A_i to all points in the curved sector; this way, for i>1 the weight of any point $p\in S_i$ is within factor $1+\varepsilon$ of the area of the triangle pqr:

$$|pqr| \le A_i \le (1+\varepsilon)|pqr| \qquad \forall p \in S_i, \forall i > 1$$
 (3)

For every cell σ of the visibility decomposition, we overlay the level sets from each of the O(n) triangles of V(p) for $p \in \sigma$. We confine the level sets to the cell, i.e., for each curve γ_A use only the intersection $\gamma_A \cap \sigma$. We call each cell of the overlay a *region* and set the weight of the region to the sum of the weights of the curved sectors whose intersection forms the region.

To bound the number of level sets used (i.e., to determine the first area A_1 in the geometric sequence \mathcal{A} and the needed length of the sequence), assume that vertices of P have integer coordinates and let L denote the largest coordinate. (This model and its variants are common for WRP; in particular, the running times of known solutions for WRP [2,7–9,21,31] depend on L.) Now, consider a triangulation T of P – any point $p \in P$ lies inside a triangle τ of T and sees all of the triangle; thus the area |V(p)| is at least the area of τ , which, by Pick's Theorem is at least 1/2:

$$|V(p)| \ge 1/2\tag{4}$$

We are now ready to prove that it suffices to have

$$A_1 = \frac{\varepsilon}{2n} \tag{5}$$

Indeed, suppose V(p) consists of K triangles of areas $\Delta_1, \ldots, \Delta_K$ and let A_1, \ldots, A_K be the weights of the curved sectors that formed the region to which p belongs; the weight of the region is thus $w(p) = A_1 + \cdots + A_K$. Classify the triangles as "small" and "large", with the former having area at most A_1 (and thus having p lie in the sector S_1) and the latter having area larger than A_1 (with p in a sector S_i for i > 1); let $l = \{k : \Delta_k > A_1\}$ be the indices of the large triangles. By (3), for every large triangle $k \in l$, $A_k \leq (1 + \varepsilon)\Delta_k$. Since $K \leq n$, we have

$$w(p) = \sum_{k \in l} A_k + \sum_{k \notin l} A_k \le (1 + \varepsilon) \sum_{k \in l} \Delta_k + nA_1 \le (1 + \varepsilon)|V(p)| + \varepsilon \frac{1}{2} \le (1 + 2\varepsilon)|V(p)|$$
 (6)

where the last inequality is due to (4).

▶ Proposition 1. If WRP on N regions with curved boundaries of constant algebraic complexity can be $(1+\varepsilon)$ -approximated in time $T(N,\frac{1}{\varepsilon})$, then a $(1+\varepsilon)^2$ -approximation to the minimum integral exposure path can be found in time $T(\frac{n^{10}}{\varepsilon^2}\log^2(nL),\frac{1}{\varepsilon})$.

Proof. For an upper bound on the sector weight, note that obviously $\forall p \in P, |V(p)| \leq L^2$. Hence, the number of needed level sets is at most $\log_{1+\varepsilon}(2nL^2) = O(\frac{1}{\varepsilon}\log(nL))$. The level sets are defined for each of the $O(n^3)$ triples r', q', \bar{qr} where r', q' are vertices and \bar{qr} is the side of P containing qr; thus overall there are $O(\frac{n^3}{\varepsilon}\log(nL))$ level set curves. Since each

curve γ_A has constant algebraic degree (cf. (2)), the complexity of the overlay of the level sets inside the cell σ of the visibility decomposition is $O((\frac{n^6}{\varepsilon})^2 \log^2(nL))$. Since there are $O(n^4)$ cells, our construction splits P into $O(\frac{n^{10}}{\varepsilon^2} \log^2(nL))$ regions of constant weight.

By (6), region weights approximate the visibility area to within $1+\varepsilon$ (use $\varepsilon:=\varepsilon/2$ to get rid of the factor 2 in front of ε); hence finding a $(1+\varepsilon)$ -approximate solution to the WRP on our regions provides a $(1+\varepsilon)^2$ -approximation to the minimum integral exposure path. Formally, let π^* be the minimum integral exposure path (the optimal solution to INTEGRAL GEOMETRIC SECLUDED PATH), let $\bar{\pi}$ be the minimum-weight path through our regions (the optimal solution to WRP) and let π be the $(1+\varepsilon)$ -approximate solution to WRP; then

$$\int_{\pi} |V(p)| \, \mathrm{d}p \le \int_{\pi} w(p) \, \mathrm{d}p \le (1+\varepsilon) \int_{\bar{\pi}} w(p) \, \mathrm{d}p \le (1+\varepsilon) \int_{\pi^*} w(p) \, \mathrm{d}p \le (1+\varepsilon)^2 \int_{\pi^*} |V(p)| \, \mathrm{d}p$$

$$\tag{7}$$

where the first inequality is due to the left inequality of (3), the second is because π approximates $\bar{\pi}$, the third is because $\bar{\pi}$ is optimal w.r.t. w, and the last one is due to the right inequality in (3).

3.2 A detailed implementation

Applicability of Proposition 1 remains questionable due to absence of an algorithm for WRP with curved regions boundaries. In this section we present another, direct approach to reduce our problem to WRP on a *polygonal* subdivision. We refine the visibility decomposition (without affecting the asymptotic complexity) and recalculate the area functions so that they have *linear* levels. This way, the regions in the overlay of the level sets are convex, so existing WRP solutions can be applied directly.

Specifically, we differentiate between fixed-endpoint and rotating sides of the triangles into which V(p) is split: the former end at a vertex of P while the latter rotate around a vertex if p moves (see Fig. 4, left). Triangles whose both sides are fixed-endpoint are easy to handle: (while the area of each individual triangle changes as p moves,) the *total* area of all such triangles remains the same (moving p just redistributes the area between the triangles, "stealing" from some and "giving" to others). We therefore call such triangles fixed.

Consider now a triangle pqr whose both sides pq, pr are rotating around vertices q', r' resp. (this is the most general case: if one of the sides, say, pq' is fixed, we can just assume q=q'); assume that rq is horizontal (Fig. 5, left). We refine the visibility decomposition by extending the vertical segments through each of r', q' maximally up and down; let R, Q be the feet of the perpendiculars dropped from r' and q' resp. onto the supporting line of pq (any of r'R, q'Q may lie only partially inside P, as in Fig. 5, right – this is not an issue). Note that |Rr'pq'Q| may be added to the fixed-triangles areas – the total area of all fixed triangles plus the areas of the pentagons Rr'pq'Q for all the triangles with p as the apex does not depend on p. Denote this total area by C. The area |V(p)| is obtained from C by adding/subtracting the areas of the triangles r'Rr for all vertices r' on which a side of a triangle of V(p) rotates – whether |r'Rr| is added or subtracted depends on whether the triangle is in V(p) or not:

$$|V(p)| = C + \sum_{r' \in \oplus} \Delta_r - \sum_{r' \in \ominus} \Delta_r \tag{8}$$

where $\Delta_r = |r'Rr|$ and \oplus (resp. \ominus) is the set of vertices whose triangles r'Rr are visible (resp. invisible) from p.

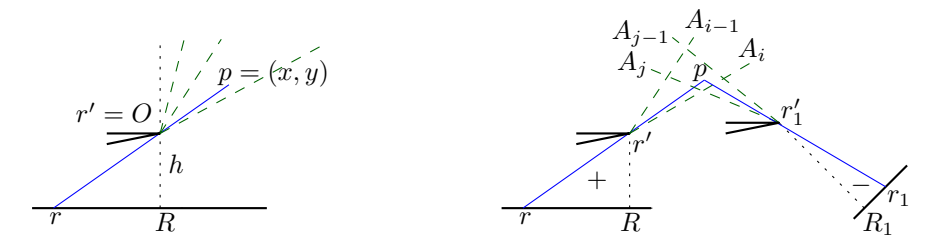


Figure 6 Left: Green dashed are level sets of the area function Δ_r (9). Right: A_i contributes positively to w(p) while A_j comes with minus into w(p), because for p in this region, $r' \in \oplus (r'Rr \in V(p))$ while $r'_1 \in \ominus (r'_1R'r'_1 \notin V(p))$.

Assume that r' is the origin O and that the supporting line of rR is the horizontal line y = -h, and let p = (x.y) with $x \ge 0$ (Fig. 6, left). Then

$$\Delta_r = \frac{h^2}{2} \frac{x}{y} \tag{9}$$

and a level set $\gamma_A = \{p = (x,y) : \Delta_r = A\}$ of the function (9) is a ray (emanating from the origin) of constant x/y: since the height r'R of the triangle is fixed, Δ_r is constant whenever r is fixed. As in Section 3.1, we draw the rays for a set $\mathcal{A} = (A_1, \ldots, A_i, \ldots)$ of areas forming geometric progression with common ratio $1+\varepsilon$ and assign the weight A_i to all points in the sector $S_i = \{p \in \sigma : A_{i-1} < \delta_r \leq A_i\}$ between $\gamma_{A_{i-1}}$ and γ_{A_i} (we again use the weight $A_1 = \varepsilon/(2n)$ for points between γ_0 and γ_{A_1}). Also as in Section 3.1, we define a region as a cell in the overlay of the rays emanating from the vertices r' of P. Finally, the weight w(p) any point p in a region is determined by C and the weights of the sectors forming the region: for a vertex $r' \in \oplus$ the weights of the sectors of r' are added to regions weights; for a vertex $r' \in \oplus$, the weights are subtracted (Fig. 6, right).

The fact that our subdivision into regions provides a $(1+\varepsilon)$ -approximation to |V(p)| can be argued similarly to Section 3.1; see Appendix A for the formulas:

▶ Theorem 3. If WRP on N regions can be $(1+\varepsilon)$ -approximated in time $T(N, \frac{1}{\varepsilon})$, then a $(1+\varepsilon)^3$ -approximation to the minimum integral exposure path can be found in time $T(\frac{n^4}{\varepsilon}\log(nL), \frac{1}{\varepsilon})$.

We conclude the section with several remarks on the complexity of our solution:

- A faster algorithm for our problem could potentially be obtained by using a "1D" discretization of edges of the visibility decomposition (instead of creating a 2D "grid" of regions, as we do), as done in many algorithms for WRP (and related problems on minimizing path integral [1,42]). Such a solution, however, would require knowing the optimal path connecting points on the boundary of the same cell of the decomposition. This, may be quite complicated, as it amounts to minimizing the integral of a function with $\Omega(n)$ terms, for which an analytical solution might not exist (though an approximation may be possible).
- An algorithm for WRP with regions whose boundaries are curves of constant algebraic degree could be interesting and would lead to a solution of our problem just using the generic scheme from Section 3.1. The biggest stumbling block for the design of such an algorithm may be the non-convexity of the regions, implying that a segment between two points on the boundary of a region is not guaranteed to stay inside the region. It may be possible that WRP techniques could be adapted to handle our regions from Section 3.1 by approximating their boundaries with piecewise-linear functions (since we are looking



Figure 7 Shortest s-t path (solid) sees the niches behind s and t for its whole length; stepping to the side (dashed path) decreases the integral exposure.

- only for a $(1+\varepsilon)$ -optimal path, the fineness of such piecewise-linear approximation would also be controlled by ε).
- Since our problem is an extension of WRP to the case of continuously changing weight, it may be tricky to establish hardness of the problem, as the complexity of WRP has remained open for many years (see [11] for a recent proof of algebraic complexity of WRP). Differently from 0/1 exposure (Theorem 3), even in simple polygons the shortest path does not necessarily minimize the integral exposure (Fig. 7, right).

On planar optimal satisfiability

In this section we return to the (non-integral) Geometric Sectuded Path problem (Section 2) and elaborate on its connections to planar satisfiability, identifying, in particular, polynomially solvable and hard versions of planar minSAT and maxSAT. In Section 4.1 we discuss connections of Geometric Sectuded Path to the graph version of the Sectuded Path problem.¹

For a SAT instance with variables V and clauses C, the graph $G = (V \cup C, E)$ of the instance is the bipartite graph whose parts are the variables and the clauses, and whose edges connect each variable to a clause whenever the variable or its negation appears in the clause. In a planar SAT, G is planar. Planar SAT has been the staple starting point for hardness reduction in computational geometry. In many cases, hardness of geometric problems was proved using restricted hard versions of planar SAT, such as:

V-cycle SAT: G remains planar after adding a cycle through V (G is no longer bipartite)

VC-cycle SAT: G remains planar after adding a cycle through $V \cup C$ (this version, as well as V-cycle SAT were defined already in the original paper on planar SAT [26])

Separable SAT: A further restriction of V-cycle SAT: for any variable x, the V-cycle separates clauses containing x from the clauses containing \overline{x} ; in other words, no variable x has an x-containing clause and a \overline{x} -containing clause on the same side of the V-cycle (this version is from [26, Lemma 1], but has no name there; we take the name from [37])

Monotone SAT: In any clause, all variables are either non-negated or all variables are negated (this version is defined for general, not only for planar SAT)

See [12,37] for in-depth treatment of restricted planar SAT versions and their uses.

When proving hardness of Geometric Secluded Path in Section 2 (Theorem 1) we spent considerable effort on dealing with crossings between variable–clause connectors. A natural question is why we did not reduce from planar minSAT. The answer is that to avoid crossings, our reduction should better start from separable minSAT (Fig. 8, left), so that for any variable x, the connections from literal x reside on one side of the Christmas tree

¹ Some content in this section is of "negative" type—why things do not work—which may still be interesting, as, in particular, it shows which approaches are doomed when trying to prove hardness of Secluded Path in planar graphs (an open problem, to our knowledge).

B

 $\overline{x_1} \vee x_2$

 $x_2 \vee \overline{x_3}$

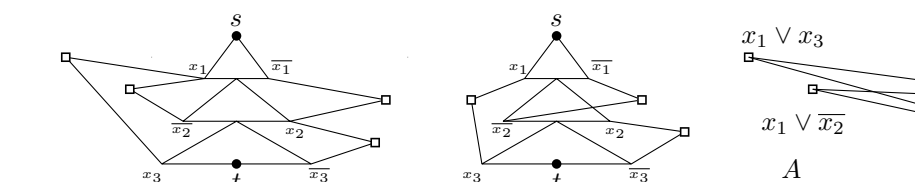


Figure 8 Left: Reduction from separable minSAT to GEOMETRIC SECLUDED PATH would have no crossings (note that some variables have their negations on one side of the Christmas tree, while others – on the other; this is fine, since the definition of separable SAT requires separability locally for each variable; the separability does not have to be consistent across all variables). Middle: In non-separable minSAT, clause $\overline{x_1} \vee \overline{x_2}$ could be seen not only from s-t path via $\overline{x_2}$ but also from s-t path via x_2 due to the crossing with the Christmas tree. Right: the graph H (which happens to be $K_{2,2}$) for the instance on the left.

and the connections from \overline{x} – on its other side (otherwise, a connection from, say, \overline{x} would cross the Christmas tree itself; Fig. 8, middle). However:

▶ **Theorem 4.** Separable minSAT can be solved in polynomial time.

Proof. Let A be the clauses on one side of the variable chain and $B = C \setminus A$ – the clauses on the other side. Construct the "clause conflict" graph H [28] whose vertices are the clauses and whose edges connect two clauses whenever one contains the negation of a literal in the other (Fig. 8, right). For any edge, at least one of the conflicting clauses will be satisfied in any truth assignment; thus, every edge in the graph will be incident to a satisfied clause. In particular, solving the minSAT is equivalent to finding minimum vertex cover (VC) in H. By the separability, for any variable x, all clauses with x are in A and all clauses with x are in x and the variable x any edge of x connects a clause in x with a clause in x is bipartite, and the vC in it can be found in polynomial time.

Note that the above proof does not use the planarity. In particular, monotone minSAT can be solved similarly: the clauses with all positive variables can form the set A and the clauses with all negative variables – set B in the graph H from the proof. We thus have:

▶ Corollary 5. Monotone minSAT (planar or not) can be solved in polynomial time.

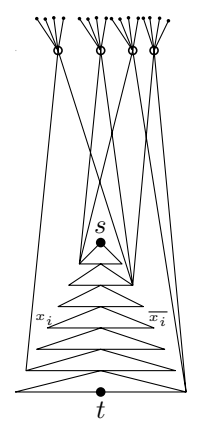
In Appendix C we prove NP-hardness of V-cycle min2SAT (we leave hardness of VC-cycle minSAT open), as well as hardness of all four versions of planar max2SAT (these do not have relation to secluded paths; we give the proofs just for completeness of our treatment of planar optSAT):

▶ **Theorem 6.** The following planar versions of max2SAT are NP-hard: V-cycle, VC-cycle, monotone, separable. V-cycle min2SAT is NP-hard.

4.1 Secluded paths in graphs

Recall that in Secluded Path (the original, graph problem) the goal is to find an *s-t* path adjacent to fewest vertices of the graph (vertices of the path itself are also counted as adjacent to the path). The problem was proved hard in [6]. Our proof of hardness of Geometric Secluded Path (Theorem 1) gives an alternative proof of hardness of Secluded Path in graphs: simply remove equalizers and leakage-blocking chambers from Fig. 1 (no need to care about midway intersections and all the other geometric technicalities) and add a large number of extra vertices adjacent to each clause vertex (Fig. 9, left). While our proof

XX:12 Geometric secluded paths and planar satisfiability



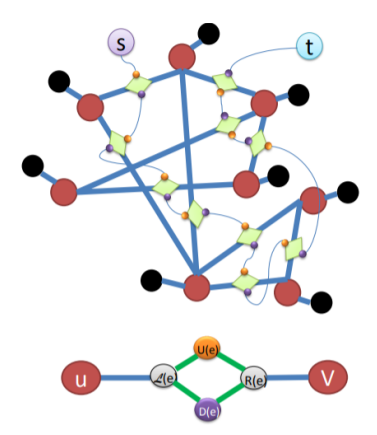


Figure 9 Left: Our reduction from min2SAT to SECLUDED PATH. To avoid high-degree vertices at the clauses (hollow), s-t path will go via the Christmas tree, setting the variables; the number of seen (i.e., adjacent) clause vertices is the number of satisfied clauses. Right: The reduction from VC in a graph G [6, Fig. 3]: the new graph G' has new vertices s and t, and an s-t path (thin blue) crossing all edges (thick blue) is added to G, with every crossing (lightgreen rhombi) turned into a gadget (bottom) where s-t path chooses which vertex of G (red) the path will see; leaking into the original vertices of G (red) is prevented in G' by attaching high-weight vertices (black).

is simpler than the ones in [6], it is less powerful because Chechik et al. [6] showed also hardness of approximation. In fact, the reduction in [6], shown here on Fig. 9, right, may also be seen as reduction from minSAT (in view of the connection between minSAT and VC in the clause conflict graph – see proof of Theorem 4): the choices that the s-t path makes in the edges of the original graph G may be seen as setting the truth values to the variables (similarly to how the path through our Christmas tree does it).

A natural question, arising in view of the effort we spent dealing with the crossings in Section 2 when proving hardness of Geometric Secluded Path (Theorem 1), is why did we not reduce from Secluded Path in planar graphs. The answer is that we are not aware of a hardness result for the problem in planar graphs. Indeed, even though Chechik et al.'s hardness proof for general graphs (refer to Fig. 9, right) could reduce from VC in a planar graph G, in order to keep the planarity also in the resulting graph G' (in which the secluded s-t path is sought), the added path (crossing all edges of G) must cross each edge exactly once, meaning that it is an Euler path in the planar dual of G, meaning that the dual has vertices of even degree only, meaning that G has faces with even number of edges, meaning it has only even cycles, meaning it is bipartite, meaning VC is polynomial in it.² Thus, likely, different techniques would be needed to prove happened of Secluded Path in planar graphs (assuming the problem is hard at all).

Acknowledgements. We thank Mike Paterson for raising the question of finding minimum-exposure paths and Erik Demaine, Jayson Lynch, Tom van der Zanden, Irina Kostitsyna, Topi Talvitie, Bengt Nilsson and Joe Mitchell for helpful discussions.

² Strictly speaking, since we need only an Euler path through the edges, not Euler cycle, G may have 2 odd faces – we believe VC is still polynomial in such graphs (e.g., if the odd cycles are triangle, the graph is perfect, implying that minimum VC in it can be found efficiently, as the complement of the max independent set)

References

- 1 Pankaj K Agarwal, Kyle Fox, and Oren Salzman. An efficient algorithm for computing high-quality paths amid polygonal obstacles. *ACM Transactions on Algorithms (TALG)*, 14(4):46, 2018.
- 2 Lyudmil Aleksandrov, Anil Maheshwari, and J-R Sack. Determining approximate shortest paths on weighted polyhedral surfaces. *Journal of the ACM (JACM)*, 52(1):25–53, 2005.
- 3 Esther M Arkin, Alon Efrat, Christian Knauer, Joseph Mitchell, Valentin Polishchuk, Günter Rote, Lena Schlipf, and Topi Talvitie. Shortest path to a segment and quickest visibility queries. *Journal of Computational Geometry*, 7(2):77–100, 2016. Special issue on SoCG'15.
- 4 Boris Aronov, Alon Efrat, Ming Li, Jie Gao, Joseph SB Mitchell, Valentin Polishchuk, Boyang Wang, Hanyu Quan, and Jiaxin Ding. Are friends of my friends too social? limitations of location privacy in a socially-connected world. In *Proceedings of the Eighteenth ACM International Symposium on Mobile Ad Hoc Networking and Computing*, pages 280–289. ACM, 2018.
- 5 Svante Carlsson, Håkan Jonsson, and Bengt Nilsson. Finding the shortest watchman route in a simple polygon. *Discrete & Computational Geometry*, 22(3):377–402, 1999.
- 6 Shiri Chechik, Matthew P Johnson, Merav Parter, and David Peleg. Secluded connectivity problems. *Algorithmica*, 79(3):708–741, 2017.
- 7 Siu-Wing Cheng, Jiongxin Jin, and Antoine Vigneron. Triangulation refinement and approximate shortest paths in weighted regions. In *Proceedings of the twenty-sixth annual ACM-SIAM symposium on Discrete algorithms*, pages 1626–1640. SIAM, 2014.
- 8 Siu-Wing Cheng, Hyeon-Suk Na, Antoine Vigneron, and Yajun Wang. Approximate shortest paths in anisotropic regions. *SIAM Journal on Computing*, 38(3):802–824, 2008.
- 9 Siu-Wing Cheng, Hyeon-Suk Na, Antoine Vigneron, and Yajun Wang. Querying approximate shortest paths in anisotropic regions. *SIAM Journal on Computing*, 39(5):1888–1918, 2010.
- 10 Otfried Cheong, Alon Efrat, and Sariel Har-Peled. Finding a guard that sees most and a shop that sells most. *Discrete & Computational Geometry*, 37(4):545–563, 2007.
- Jean-Lou De Carufel, Carsten Grimm, Anil Maheshwari, Megan Owen, and Michiel Smid. A note on the unsolvability of the weighted region shortest path problem. *Computational Geometry*, 47(7):724–727, 2014.
- 12 Erik Demaine. Algorithmic lower bounds: Fun with hardness proofs. MIT OCW.
- 13 Hristo N Djidjev. Efficient computation of minimum exposure paths in a sensor network field. In *International Conference on Distributed Computing in Sensor Systems*, pages 295–308. Springer, 2007.
- 14 M.E Dyer and A.M Frieze. Planar 3dm is np-complete. *Journal of Algorithms*, 7(2):174 184, 1986. URL: http://www.sciencedirect.com/science/article/pii/0196677486900027, doi:https://doi.org/10.1016/0196-6774(86)90002-7.
- 15 Hao Feng, Lei Luo, Yong Wang, Miao Ye, and Rongsheng Dong. A novel minimal exposure path problem in wireless sensor networks and its solution algorithm. *International Journal of Distributed Sensor Networks*, 12(8):1550147716664245, 2016.
- Fedor V Fomin, Petr A Golovach, Nikolay Karpov, and Alexander S Kulikov. Parameterized complexity of secluded connectivity problems. Theory of Computing Systems, 61(3):795–819, 2017.
- 17 Laxmi Gewali, Alex C. Meng, Joseph S. B. Mitchell, and Simeon C. Ntafos. Path planning in 0/1/infinity weighted regions with applications. In Herbert Edelsbrunner, editor, *Proceedings of the Fourth Annual Symposium on Computational Geometry, Urbana-Champaign, IL, USA, June 6-8, 1988*, pages 266–278. ACM, 1988.
- 18 Subir Ghosh. Visibility Algorithms in the Plane. Cambridge University Press, New York, NY, USA, 2007.

XX:14 Geometric secluded paths and planar satisfiability

- 19 J.E. Goodman and J. O'Rourke, editors. *Handbook of Discrete and Computational Geometry*. Discrete Mathematics and Its Applications. Taylor & Francis, 2nd edition, 2004.
- 20 Leonidas J Guibas, John E Hershberger, Joseph SB Mitchell, and Jack Scott Snoeyink. Approximating polygons and subdivisions with minimum-link paths. *International Journal of Computational Geometry & Applications*, 3(04):383–415, 1993.
- 21 Rajasekhar Inkulu and Sanjiv Kapoor. A polynomial time algorithm for finding an approximate shortest path amid weighted regions. *Preprint*, 2015.
- 22 Rajeev Kohli, Ramesh Krishnamurti, and Prakash Mirchandani. The minimum satisfiability problem. SIAM Journal on Discrete Mathematics, 7(2):275–283, 1994.
- 23 Irina Kostitsyna, Maarten Löffler, Valentin Polishchuk, and Frank Staals. On the complexity of minimum-link path problems. *JoCG*, 8(2):80–108, 2017. Special Issue on SoCG'16. URL: http://jocg.org/index.php/jocg/article/view/328.
- Niel Lebeck, Thomas Mølhave, and Pankaj K Agarwal. Computing highly occluded paths on a terrain. In Proceedings of the 21st ACM SIGSPATIAL International Conference on Advances in Geographic Information Systems, pages 14–23. ACM, 2013.
- Niel Lebeck, Thomas Mølhave, and Pankaj K Agarwal. Computing highly occluded paths using a sparse network. In Proceedings of the 22nd ACM SIGSPATIAL International Conference on Advances in Geographic Information Systems, pages 3–12. ACM, 2014.
- 26 David Lichtenstein. Planar formulae and their uses. SIAM journal on computing, 11(2):329–343, 1982.
- 27 Max-Jonathan Luckow and Till Fluschnik. On the computational complexity of length-and neighborhood-constrained path problems. arXiv preprint arXiv:1808.02359, 2018.
- Madhav V Marathe and SS Ravi. On approximation algorithms for the minimum satisfiability problem. *Information Processing Letters*, 58(1):23–29, 1996.
- J. Mitchell, G. Rote, and G. Woeginger. Minimum-link paths among obstacles. *Alg-ca'92*, 8(1):431–459, 1992.
- 30 Joseph Mitchell, Valentin Polishchuk, and Mikko Sysikaski. Minimum-link paths revisited. CGTA, 47(6):651–667, 2014.
- 31 Joseph SB Mitchell and Christos H Papadimitriou. The weighted region problem: finding shortest paths through a weighted planar subdivision. *Journal of the ACM (JACM)*, 38(1):18–73, 1991.
- 32 Joseph O'Rourke. Art Gallery Theorems and Algorithms. The International Series of Monographs on Computer Science. Oxford University Press, New York, NY, 1987.
- 33 Christos H Papadimitriou. An algorithm for shortest-path motion in three dimensions. *Information Processing Letters*, 20(5):259–263, 1985.
- 34 Valentin Polishchuk and Leonid Sedov. Gender-aware facility location in multi-gender world. In LIPIcs-Leibniz International Proceedings in Informatics, volume 100. Schloss Dagstuhl-Leibniz-Zentrum fuer Informatik, 2018.
- 35 Yuning Song, Liang Liu, Huadong Ma, Athanasios V Vasilakos, et al. A biology-based algorithm to minimal exposure problem of wireless sensor networks. *IEEE Trans. Network and Service Management*, 11(3):417–430, 2014.
- 36 Subhash Suri. A linear-time algorithm for minimum link paths inside a simple polygon. Computer Vision, Graphics and Image Processing, 35(1):99–110, 1986.
- 37 Simon Tippenhauer and Wolfgang Muzler. On planar 3-sat and its variants. Fachbereich Mathematik und Informatik der Freien Universitat Berlin, 2016.
- 38 Csaba D Toth, Joseph O'Rourke, and Jacob E Goodman. *Handbook of discrete and computational geometry*. Chapman and Hall/CRC, 2017.
- 39 René van Bevern, Till Fluschnik, and Oxana Yu. Tsidulko. Parameterized algorithms and data reduction for safe convoy routing. In 18th Workshop on Algorithmic Approaches for

Transportation Modelling, Optimization, and Systems, ATMOS 2018, August 23-24, 2018, Helsinki, Finland, pages 10:1–10:19, 2018.

- 40 Giacomino Veltri, Qingfeng Huang, Gang Qu, and Miodrag Potkonjak. Minimal and maximal exposure path algorithms for wireless embedded sensor networks. In *Proceedings of the 1st international conference on Embedded networked sensor systems*, pages 40–50. ACM, 2003.
- 41 Haitao Wang. Quickest visibility queries in polygonal domains. In Boris Aronov and Matya Katz, editors, 33rd International Symposium on Computational Geometry, SoCG 2017, July 4-7, 2017, Brisbane, Australia, volume 77 of LIPIcs, pages 61:1–61:16. Schloss Dagstuhl Leibniz-Zentrum fuer Informatik, 2017.
- 42 Ron Wein, Jur Van Den Berg, and Dan Halperin. Planning high-quality paths and corridors amidst obstacles. *The International Journal of Robotics Research*, 27(11-12):1213–1231, 2008.
- Ron Wein, Jur Van Den Berg, and Dan Halperin. Planning near-optimal corridors amidst obstacles. In *Algorithmic Foundation of Robotics VII*, pages 491–506. Springer, 2008.
- 44 Ron Wein, Jur P Van den Berg, and Dan Halperin. The visibility–voronoi complex and its applications. *Computational Geometry*, 36(1):66–87, 2007.

A Formalities omitted from Section 3.2

For a point $p \in P$, split the areas Δ_r from (8) into large (larger than A_1) and small (the others). By construction, the area Δ_r of every large triangle r'Rr is $(1+\varepsilon)$ -approximated by the weight A_i of the sector S_i (i > 1) to which p belongs

$$\Delta_r \le A_i \le (1+\varepsilon)\Delta_r \tag{10}$$

while for small Δ_r

$$0 \le \Delta_r \le A_1 \tag{11}$$

In particular, since there are at most n small triangles, their total area is at most $nA_1 = \varepsilon/2 \le \varepsilon |V(p)|$ (cf. (4)); thus replacing Δ_r with A_1 for each small triangle changes |V(p)| by at most an additive $\varepsilon |V(p)|$.

Formally, let $\oplus_1 \subseteq \oplus$ (resp. $\ominus_1 \subseteq \ominus$) denote the vertices in \oplus (resp. \ominus) for which Δ_r is small. We can expand (8) into

$$|V(p)| = C + \sum_{r' \in \oplus \backslash \oplus_1} \Delta_r + \sum_{r' \in \oplus_1} \Delta_r - \sum_{r' \in \ominus \backslash \ominus_1} \Delta_r - \sum_{r' \in \ominus_1} \Delta_r$$
(12)

The weight w(p) is obtained by replacing Δ_r in each summand with the area A_i of the sector $S_i \ni p$:

$$w(p) = C + \sum_{\oplus \backslash \oplus_1} A_i + \sum_{\oplus_1} A_1 - \sum_{\ominus \backslash \ominus_1} A_i - \sum_{\ominus_1} A_1$$
 (13)

Using (10) and (11), we get

$$w(p) \le C + (1+\varepsilon) \sum_{r' \in \oplus \backslash \oplus_1} \Delta_r + \varepsilon |V(p)| - \sum_{r' \in \ominus \backslash \ominus_1} \Delta_r - \sum_{r' \in \ominus_1} \Delta_r$$
 (14)

Observe that even if the triangles from \oplus are removed from V(p), the point p still sees a non-negative area, i.e.,

$$C - \sum_{r' \in \ominus \backslash \ominus_1} \Delta_r - \sum_{r' \in \ominus_1} \Delta_r \ge 0$$

XX:16 Geometric secluded paths and planar satisfiability

which means that

$$C - \sum_{r' \in \Theta \setminus \Theta_1} \Delta_r - \sum_{r' \in \Theta_1} \Delta_r \qquad \leq \qquad (1 + \varepsilon) \left(C - \sum_{r' \in \Theta \setminus \Theta_1} \Delta_r - \sum_{r' \in \Theta_1} \Delta_r \right)$$

Substituting this into (14) and comparing with (12), we get

$$w(p) \le (1+2\varepsilon)|V(p)|$$

On the other hand, from (10)-(13),

$$w(p) \ge C + \sum_{\oplus \backslash \oplus_1} \Delta_r + \sum_{\oplus_1} \Delta_r - (1+\varepsilon) \sum_{\ominus \backslash \ominus_1} \Delta_r - \sum_{\ominus_1} \frac{\varepsilon |V(p)|}{n} \ge$$

$$\ge C + \sum_{\oplus \backslash \oplus_1} \Delta_r + \sum_{\oplus_1} \Delta_r - \sum_{\ominus \backslash \ominus_1} \Delta_r - \varepsilon \sum_{\ominus \backslash \ominus_1} \Delta_r - \varepsilon |V(p)| \ge$$

$$\ge C + \sum_{\oplus \backslash \oplus_1} \Delta_r + \sum_{\oplus_1} \Delta_r - \sum_{\ominus \backslash \ominus_1} \Delta_r - \sum_{\ominus_1} \Delta_r - \varepsilon \sum_{\ominus \backslash \ominus_1} \Delta_r - \varepsilon |V(p)| \ge$$

$$\ge |V(p)| - \varepsilon |V(p)| - \varepsilon |V(p)| = (1 - 2\varepsilon) |V(p)|$$

Similarly to (7), the above proves the approximation ratio:

$$\int_{\pi} w(p) dp \leq \frac{(1+2\varepsilon)(1+\varepsilon)}{1-2\varepsilon} \int_{\pi^*} |V(p)| dp$$

where π is the $(1+\varepsilon)$ -approximate path through our weighted regions and π^* is the path with minimum integral exposure.

Overall, in comparison with Section 3.1, the regions in our WRP now have straightline boundaries, so a standard WRP algorithm can be applied. Also, the number of regions is decreased, because a sequence \mathcal{A} of the level sets is defined by a $pair\ r', \bar{r}$ where r' is a vertex of P and \bar{r} is the side of P containing r; thus overall there are $O(\frac{n^2}{\varepsilon}\log(nL))$ level sets. The level sets are overlaid with the $O(n^2)$ extensions of the visibility graph edges, defining the visibility decomposition (we let the level sets straddle through the cells of the visibility decomposition since the level sets are the same irrespective of the cell; the only term in formula (8) for |V(p)| that changes from cell to cell is C). Thus overall there are $O(\frac{n^4}{\varepsilon}\log(nL))$ regions and similarly to Proposition 1 we have:

▶ **Theorem 3.** If WRP on N regions can be $(1+\varepsilon)$ -approximated in time $T(N, \frac{1}{\varepsilon})$, then $a \ (1+\varepsilon)^3$ -approximation to the minimum integral exposure path can be found in time $T(\frac{n^4}{\varepsilon}\log(nL), \frac{1}{\varepsilon})$.

Mathematica listing

$$\begin{aligned} &\inf[3]= \text{ $Assumptions } = c > 1 \text{ $\&$ } n > 0 \text{ $\&$ } h > 0 \\ &a = Sin[2*ArcTan[H+n*h,n]] \\ &i = Sin[ArcTan[\left(H*\left(1-1/\left(2*\left(c-1\right)\right)\right)\right)/h-n,\ h*n+H\right] - \\ &ArcTan[H/h-n+1,\ h*\left(n-1\right)+H]] \\ &r = i/a \\ &Limit[r,H->Infinity] \\ &FullSimplify[TrigExpand[r]] \\ &\text{Out}[13]= c > 1 \text{ $\&$ } n > 0 \text{ $\&$ } h > 0 \\ &\text{Out}[14]= Sin[2 ArcTan[H+hn,n]] \\ &\text{Out}[16]= -Sin[ArcTan[1+\frac{H}{h}-n,H+h\left(-1+n\right)] - ArcTan[\frac{\left(1-\frac{1}{2\left(-1+c\right)}\right)H}{h}-n,H+hn]] \\ &\text{Out}[16]= -Csc[2 ArcTan[H+hn,n]] \\ &Sin[ArcTan[1+\frac{H}{h}-n,H+h\left(-1+n\right)] - ArcTan[\frac{\left(1-\frac{1}{2\left(-1+c\right)}\right)H}{h}-n,H+hn]] \\ &\text{Out}[17]= \infty \\ &\text{Out}[18]= \left(H\left(H^2+2hHn+\left(1+h^2\right)n^2\right)\left(H+h\left(-5+4c+n\right)\right)\right)/ \\ &\left(2\left(-1+c\right)h\sqrt{\left(H+h\left(-1+n\right)\right)^2+\left(1+\frac{H}{h}-n\right)^2}n\left(H+hn\right) \\ &\sqrt{\left(4+\frac{\left(3-2c\right)^2}{\left(-1+c\right)^2h^2}\right)H^2+\frac{4\left(3-2c+2\left(-1+c\right)h^2\right)Hn}{\left(-1+c\right)h}+4\left(1+h^2\right)n^2} \end{aligned} \right. \end{aligned}$$

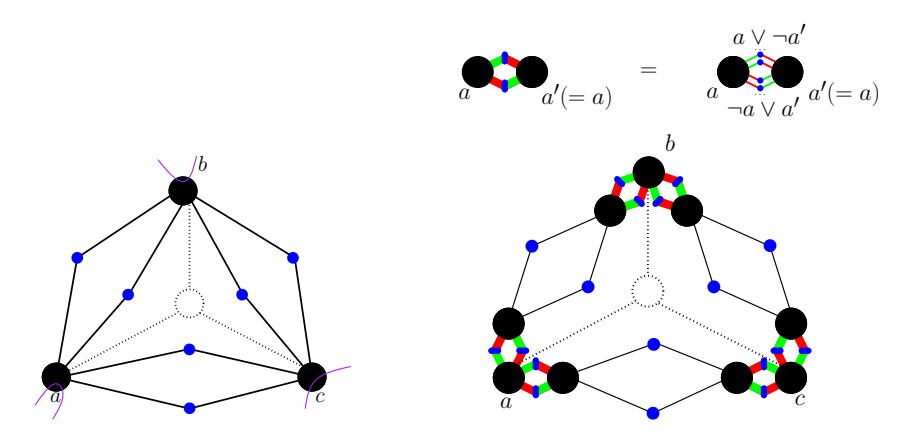


Figure 10 Left: Variables are large black disks and the six 2-literal clauses of max2SAT are blue circles; the 1-in-3SAT clause and connection to it are dotted. The V-cycle is blue. Right: Each thick red-green rhombus is the "truth propagator", consisting of the 2N clauses. Green are positive connections, red are negative.

C Hard planar versions of min2SAT and max2SAT

We prove Theorem 6, restated also here:

▶ **Theorem 6.** The following planar versions of max2SAT are NP-hard: V-cycle, VC-cycle, monotone, separable. V-cycle min2SAT is NP-hard.

Proof. Planar min2SAT (without V- or VC-cycle) was proved hard by Guibas et al. in [20, Theorem 3.2] using a reduction from planar 3SAT. We did not see how to add the cycles on top of Guibas et al.'s gadgets, and therefore present a different reduction. Some clauses in our 2SAT instances will have 1 literal (not 2) – we do not differentiate between versions of 2SAT with *exactly* 2 literals per clause and *at most* 2 literals per clause (refer to [12,37] for discussion of the differences between the versions, definitions, hardness proofs and uses of the many versions of satisfiability). We also do not show 1-literal clauses on pictures of our gadgets below, since it is straightforward to add them and extend the cycles to run through them.

To prove hardness of max2SAT with V-cycle, we reduce from V-cycle 1-in-3SAT (find truth assignment to satisfy exactly one literal in each clause) shown hard by Dyer and Frieze [14].³ We replace every clause $a \lor b \lor c$ with 9 clauses: $\neg a, \neg b, \neg c, \neg a \lor \neg b, \neg b \lor \neg c, \neg a \lor \neg c, a \lor b, b \lor c, a \lor c$. If none, 2 or 3 of a, b, c are true, then 6 new clauses are satisfied, if 1 is true - 7 are satisfied, and if all of a, b, c are true - 3 new clauses are satisfied. That is, 7|C| clauses are satisfied in the max2SAT instance iff all |C| clauses are satisfied in the 1-in-3SAT. Figure 10, left shows that if the 1-in-3SAT instance is planar, then the max2SAT instance is also planar; since the two instances have the same variables, the V-cycle in 1-in-3SAT is inherited by the max2SAT.

To prove hardness of max2SAT with VC-cycle, we reduce from VC-cycle 1-in-3SAT, also shown hard in [14]. We start from the gadget we used to prove hardness of V-cycle max2SAT (Fig. 10, left) and extend it by adding 2 copies of each of a, b, c (Fig. 10, right). The copy a' of a forms N clauses $a \lor \neg a'$ and N clauses $\neg a \lor a'$; the number N is chosen so large

³ Interestingly, Dyer and Frieze reported that they did not need the cycles for their purposes, but a referee insisted that others might need it later.

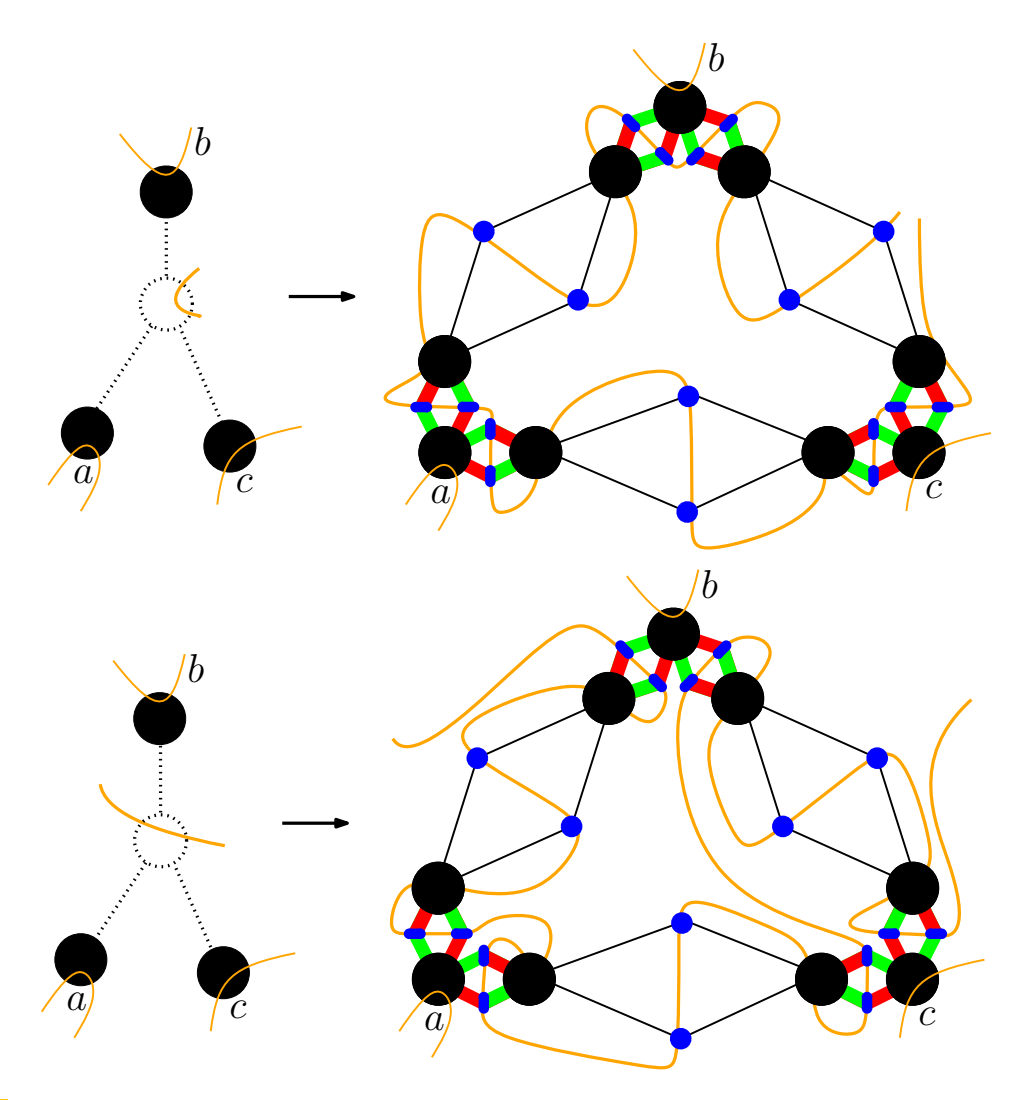


Figure 11 The VC-cycles are orange. Left: 1-in-3SAT. Right: max2SAT.

that irrespectively of the rest of the instance, the optimal truth assignment would rather set a=a' (which will satisfy all 2N clauses) than set $a=\neg a'$ (which will satisfy only N). The same is done with the remaining 5 copies (the other copy of a, 2 copies of b and 2 copies of c). Now, all |C| clauses can be satisfied in 1-in-3SAT iff 7|C|+12N|C| clauses can be satisfied in the max2SAT. Finally, note that the VC-cycle in the 1-in-3SAT instance can go through the clause either as in Fig. 11, top left (not separating the variables) or as in Fig. 11, bottom left (separating the variables); Fig. 11, right shows how to run the cycle through the new variables and clauses of max2SAT in both cases.

Next, we prove hardness of planar monotone max2SAT by reduction from planar max2SAT, resolving non-monotone clauses one-by-one as shown in Figure 12: in each non-monotone clause $x \vee \neg y$ we select one of the variables, say y, and split it into three variables y, z, t so that $y = \neg z = t$ (the same trick as above, of introducing a large number N of "parallel" monochromatic clauses $a \vee b$ and $\neg a \vee \neg b$ as the negator, is used to enforce $y = \neg z = t$ in the optimal truth assignment), and replace $x \vee \neg y$ with $x \vee z$ (t is used to pick up all the clauses on the other side of the fixed, monotonized connection). We prove hardness of sep-

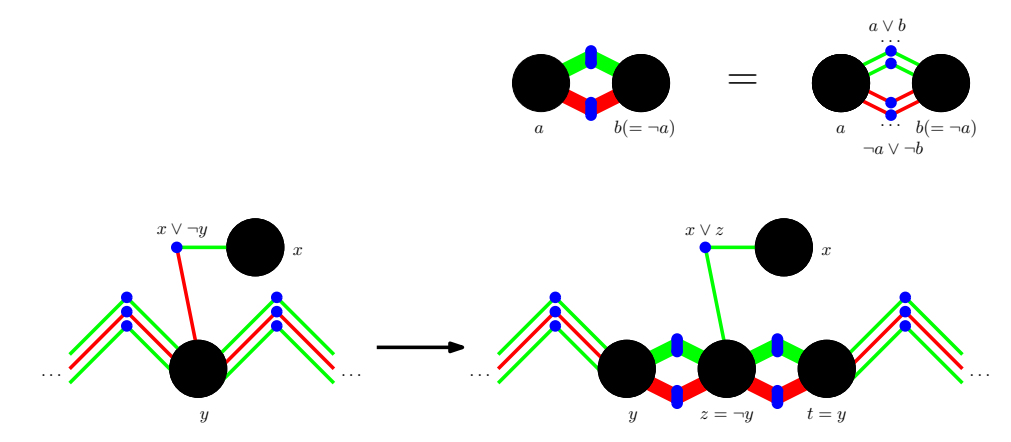


Figure 12 The monotonicity gadget. We make the clauses monochromatic one by one. As in the truth propagator in Fig. 10, every thick edge in the negator is a large number of identical connections.

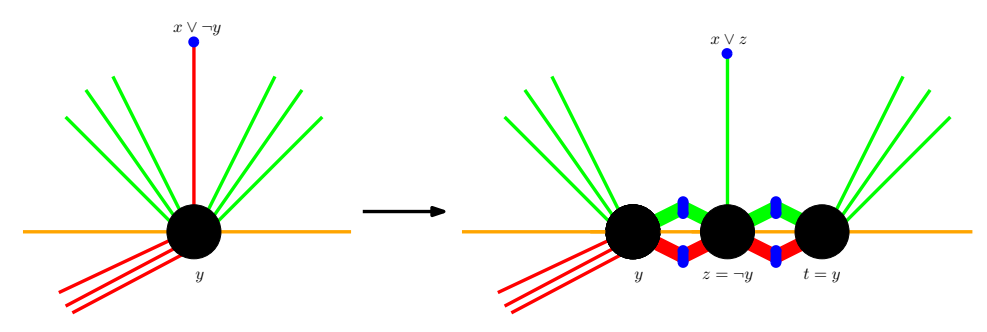


Figure 13 The separability gadget; V-cycle is orange.

arable max2SAT by reduction from planar max2SAT with V-cycle, using the same idea as in proving hardness of monotone planar min2SAT: for any variable y that has both positive and negative connections on both sides of the V-cycle, we select one side to be "positive" and the other to be "negative", and if there are negative connections on the positive side, we split y into three variables $y = \neg z = t$ and fix the connection as shown in Figure 13.

Finally, we show hardness of V-cycle min2SAT. The hardness of (non-planar) min2SAT was originally shown by Kohli et al. [22] by the following reduction from (non-planar) max2SAT: replace every clause $x \vee y$ with two clauses $\neg x \vee w, \neg y \vee w$, where w is a new variable; as is easy to see, in the new instance it is possible to satisfy at most 2|C|-k clauses iff it was possible to satisfy at least k clauses in the original instance (|C| stands for the number of clauses in the original max2SAT instance). The reduction is easy to do in a planarity-preserving way (Fig. 14); moreover, if we start from VC-cycle max2SAT, its VC-cycle becomes the V-cycle in min2SAT.

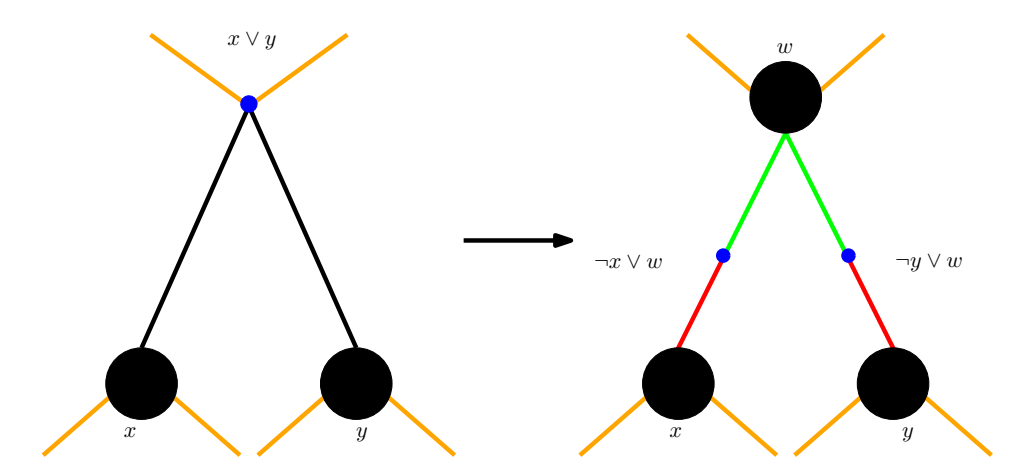


Figure 14 The planarity gadget. Left: orange is the VC-cycle in max2SAT. Right: Orange is the V-cycle in min2SAT.